The Pennsylvania State University

The Graduate School

College of Engineering

ANALYSIS AND DEVELOPMENT OF MICROSTRIP INTERDIGITATED STRUCTURES USING FDTD AND STATISTICAL TECHNIQUES

A Thesis in

Electrical Engineering

by

José G. Colom

© 1998 José G. Colom

Submitted in Partial Fulfillment
of the Requirements
for the Degree of

Doctor of Philosophy

August 1998

ABSTRACT

An analysis of two different microstrip interdigitated couplers is presented in this work. First, the well known Lange coupler is analyzed using FDTD and statistical techniques. By breaking the symmetry of the Lange coupler, a set of pre-determined values is assigned to the different physical parameters of the structure, and a metamodel is created. With the use of the metamodel, in combination with statistical graphical techniques, an optimum design point is rapidly identified. The results show that by breaking the symmetry of the coupler, there is still room to improve the output response of the circuit. The analysis was performed for a prototype Lange coupler fabricated in the lab, and for a more practical case using FDTD techniques. In both cases it was shown that a better output response is possible if the design is moved away from the nominal input settings.

A second interdigitated coupler was also developed in the lab using multilayer techniques. The design is inspired by the "unfolded" Lange coupler version, which works essentially the same as the regular Lange coupler. The new multilayer structure presents some fabrication advantages over the regular Lange coupler which makes it attractive for mass production. The new structure does not require the use of bonding wires, and limitations to line widths and spacings are not as strict as for the regular Lange coupler case. The multilayer structure could replace the Lange coupler since it was shown here that the performance of both is essentially the same. An analysis similar to the first part, using FDTD and statistical techniques, is also presented for the new structure. A commercially available Lange coupler was selected to develop a multilayer equivalent structure and compare the results. After the statistical analysis was performed, it was demonstrated that an optimum design for the multilayer case provides as good or better performance than the regular Lange coupler.

5. Microstrip Circuit Analysis Using FDTD

With the fast development of high performance workstation computers and the advent of the Pentium Pro chip in recent years, the use of expensive supercomputers to solve problems is no longer necessary. One example of such a problem is the numerical solution of a complicated microstrip structure in a three dimensional space. Microstrip structure problems are complicated to analyze in part due to the presence of the dielectric substrate. The structure is not symmetric since the metallization is placed between the dielectric and free space, therefore there is no pure TEM propagation mode and there is also possibility of radiation. One way to completely analyze the structure is using a three dimensional numerical simulation, where all the electric and magnetic fields can be calculated throughout a volume containing the microstrip circuit while observing their development in time. One of the most attractive methods that provides this type of simulation, and the main CAD tool used in this work, is the Finite Difference Time Domain or FDTD.

This method was first originated by [*Yee*, 1966] for the simulation of two dimensional electromagnetic scattering problems. His paper also presented a straight forward derivation for the more general three dimensional problem. The FDTD technique has been widely used in the past few years, and several publications provide an extensive analysis of the subject [*Kunz and Luebbers*, 1993]. The FDTD method is directly derived from discretizing the differential form of Maxwell's two curl equations. This direct application makes the code more efficient and at the same time easier to implement. Throughout the years, this method has been used to solve all kind of electromagnetic problems, and in recent years has been successfully applied to simple microstrip geometries [*Langdon* et al., submitted 1998; *Shibata and Kimura*, 1993; *Sheen* et al., 1990; *Lin and Naishadham*, 1994; *Zhao and Raisanen*, 1996; *Ko and Mittra*, 1991; *Gedney et al*. 1996; Bahr et al., 1995; *Shibata* et al., 1988]. One of the advantages of this method is that by exciting a microstrip structure with a single pulse, a large amount of information can be obtained from the resulting time domain fields. In this work, the interest is to use the frequency domain S-parameters to completely characterize the microstrip structure. It is shown later that the S-parameters can be derived from the time domain results by correctly applying the Fourier transform. Computed S-

parameters for several microstrip structures including the Lange coupler and a multilayer prototype are presented and compared to measurements in this work. The FDTD computations were obtained using XFDTD [*REMCOM*, 1997], which is a commercial UNIX-based version of the FDTD code. This software is linked to a graphics user interface (GUI) routine, which is extremely helpful when the simulation of a complicated structure is desired. XFDTD also provides the user with a selection of different parameters to compute, including the S-parameters.

5-1 FDTD Implementation

The discretization of Maxwell's two curl equations is the basis for the FDTD implementation. These two equations govern the propagation of the electromagnetic wave and they are:

$$\mu \frac{\partial \overline{H}}{\partial t} = -\nabla \times \overline{E} \tag{5.1}$$

$$\varepsilon \frac{\partial \overline{E}}{\partial t} = \nabla \times \overline{H} - \sigma \overline{E} \tag{5.2}$$

The equations can be written in Cartesian coordinates components, where a discrete approximation to the partial differential equations using centered difference approximation is applied to the time and spatial derivatives as

$$\frac{\partial f}{\partial x} \rightarrow \frac{f(x + \Delta x / 2, t) - f(x - \Delta x / 2, t)}{\Delta x} \tag{5.3}$$

$$\frac{\partial f}{\partial t} \rightarrow \frac{f(x, t + \Delta t / 2) - f(x, t - \Delta t / 2)}{\Delta t} \tag{5.4}$$

To implement the centered difference approximation, Yee defined the position of each of the six discretized field components in the FDTD rectangular unit cell or the Yee cell. This cell has dimensions $\Delta x * \Delta y * \Delta z$ and the electric and magnetic fields locations are interleaved by half of the discretization length ($\Delta x/2$, $\Delta y/2$, and $\Delta z/2$). This arrangement of fields is necessary to obtain the centered difference

approximations to the spatial derivatives. In a similar manner, by alternatively calculating the electric and magnetic fields every half a time step (Δt/2), the centered difference for the time derivative is achieved. Since the space derivative is evaluated with the half time step in between the two half time steps used to compute the time derivative, this algorithm is known as the "leap frog" algorithm.

An FDTD space is created by stacking several unit cells in a rectangular volume, the desired microstrip geometry is constructed inside this volume. The microstrip circuit is reproduced in the FDTD space following the physical geometry of the structure by assigning to the unit cells the corresponding type of material from which each section of the structure is made.

The FDTD method is straight-forward and can be easily coded to use in a computer program. The discretized fields are updated each time step in the FDTD volume without the need of any complex numerical procedures. A complete FORTRAN code applying this technique is given by *Kunz and Luebbers* [1993]. In the following section several considerations in the construction of microstrip structures using FDTD are presented.

5-2 Microstrip Implementation

Figure 5.1 shows a single microstrip line inside an FDTD computational domain with total dimensions $I\Delta x * J\Delta y * K\Delta z$ (where I, J, and K are integer numbers that define the FDTD space size). The XFDTD program was used to create similar and more complicated geometries inside the FDTD space with the help of a graphical user interface. As shown in the figure, the dielectric material is set to take the lower portion of the cube, usually 10 to 20 cells when high resolution is desired. The microstrip line metallization is simulated by assigning a PEC material to the corresponding electric fields on the dielectric/air interface. To simulate the ground plane, the lowest plane of mesh edges (plane k=1) along the microstrip conductor plane is also set to a perfect conductor. The other five walls from the cube are simulated as an unbounded space by applying the Liao [*Liao* et al., 1984] absorbing outer boundary conditions (ABC). Enough space between the microstrip conductor line and the FDTD outer walls is

necessary for the proper simulation of the unbounded space. The electric field mesh locations on the surface of the substrate also receives a special treatment when they are not set to PEC. To accurately model the air/dielectric interface in the FDTD equations, these fields are assigned a dielectric constant of $(\varepsilon_r+1)/2$. It has been also observed that due to the approximation in the spatial derivative, the widths of the microstrip line simulated with FDTD are actually extended by approximately ½ a cell at each side of the line. This approximation has to be taken into account when constructing microstrip circuits with FDTD, especially when narrow line widths and spacings are present in the structure. By reducing the cell size, the spatial resolution increases and the error becomes less critical. This approximation also applies to the length of the line, yet is not as critical since the error is negligible when compared to a long line. Special care must be taken when constructing the lines to compensate for this error. For example, to simulate a 1 cm width line with Δ=0.2 cm, four cells are required instead of five. The actual FDTD width of the line can be calculated as $4*\Delta+2(\frac{1}{2}*\Delta)$. Finally, since 98% of the fields are contained within two widths of the microstrip line, a distance of $2*W$ is used in FDTD to separate the microstrip line and the FDTD walls (see Figure 5.1). Usually, the space left for the proper operation of the ABC will take care of this condition.

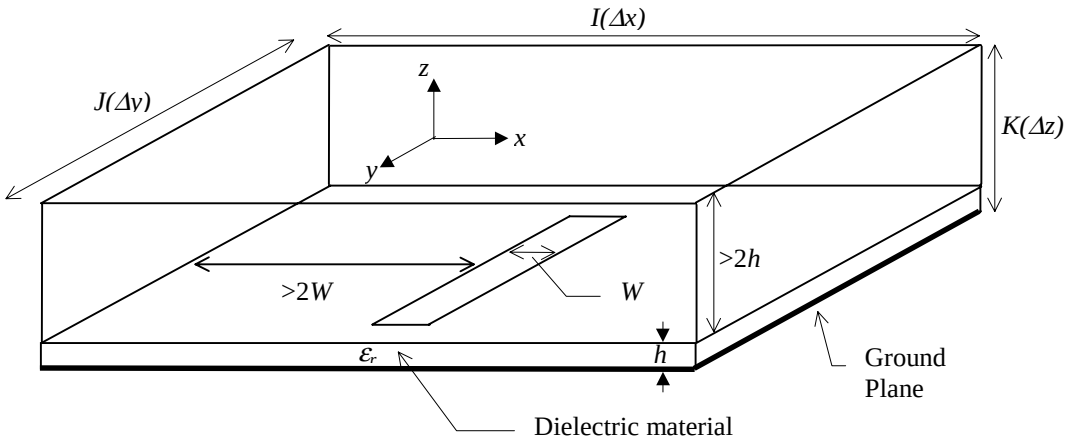

FIGURE 5.1 - FDTD space for a single microstrip line.

In XFDTD, the source location is selected by specifying the coordinates ($i_{si}\Delta x$, $j_{si}\Delta y$, $k_{si}\Delta z$) within the FDTD space. This source location is usually at the ends of the microstrip lines, this is shown in Figure 5.2 for a single microstrip line segment. The arrow in the figure represents the location of the source and the direction of the field applied.

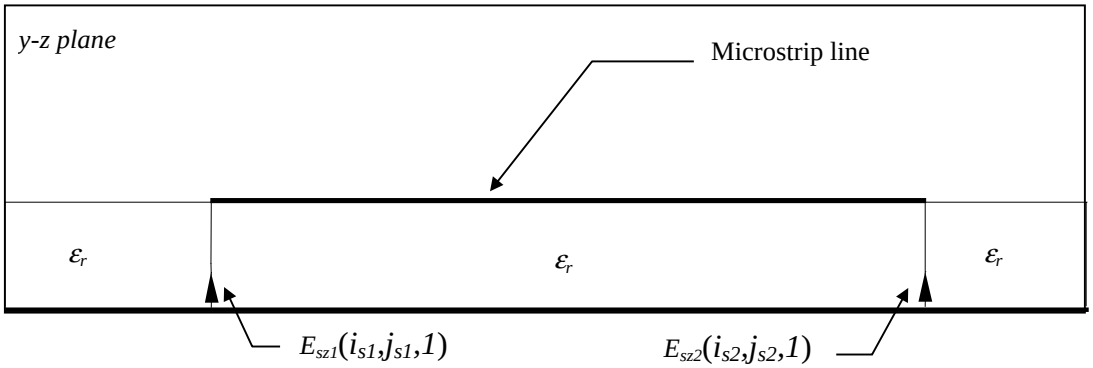

FIGURE 5.2 - Source locations in microstrip line.

In most cases, a Gaussian pulse in the +z direction is used to excite the microstrip circuit. However, if energy is trapped in the structure at undesired frequencies (this has been observed for spiral antennas and for the Lange coupler) excessive time steps can be required for the total energy release. To avoid this problem and speed up the FDTD run a modulated Gaussian pulse should be used. The frequency bandwidth and center frequency for this pulse can be controlled so that the microstrip structure is excited only at the desired frequencies. The source is usually applied by forcing a +z directed electric field on the FDTD mesh at the closest point normal to the ground plane (k=1) and centered with respect to the microstrip line width. The source is connected to the line using a simple transition.

5-3 S-Parameters Computation using FDTD

In recent years the FDTD method has been used to measure the S-parameters of different microstrip circuits. Different approaches to obtain the *S*-parameters have been presented in the literature [*Shibata and Kimura*, 1993; *Sheen* et al., 1990; *Yu*, 1997; *Lin and Naishadham*, 1994]. An approach intended to match the ports of a microstrip circuit with a lumped resistor model is discussed by Shibata and Kimura. Here the voltage and current are monitored at the ports of the circuit to be later processed and transformed to the frequency domain. The approach requires the FDTD construction of a fictitious load to terminate the ports of the structure, which is inconvenient when different cell sizes are desired to analyze the same problem.

A second approach discussed by *Sheen* et al. [1990] consists in the extension of the microstrip lines all the way to the end of the FDTD wall to use the *Mur* [1981] absorbing outer boundary as a matching load. The excitation is usually provided by a wall of distributed electric fields which is replaced by the absorbing boundaries after the pulse has been sent. At the time the method seems to work, but only after time gating undesired spurious reflections coming from the outer absorbing boundary. This method also has the disadvantage that the separation of the incident and reflected waveforms is required to calculate the S-parameters and it uses a larger FDTD space.

Recently, a simple method to measure S-parameters using FDTD was developed and presented by *Langdon* et al. [1998]. The method is easy to implement and it is more efficient than the two approaches previously mentioned. The new method is based in exciting the microstrip circuit with a voltage source that has an internal source resistance integrated into the FDTD code. The resistance has two functions; it works as a series internal resistance when a voltage source is activated, and it also works as a termination when the source is deactivated. With this approach, there is no need to construct a 50 Ω impedance to calculate the S-parameters. The implementation of an internal resistance in FDTD was previously described in [*Luebbers and Langdon*, 1996] when the excitation of a patch antenna was considered. This approach is extended by *Langdon* et al.[1998] to calculate the *S*-parameters of a multiport circuit.

The incident (a_i) and reflected (b_i) normalized voltages at each port of an N-port network can be expressed in terms of the total voltage (V_i) and total current (I_i) recorded at port *i* as

$$a_i = \frac{V_i + R_{0i} I_i}{2\sqrt{R_{0i}}} \tag{5.5}$$

$$b_i = \frac{V_i - R_{0i} I_i}{2\sqrt{R_{0i}}} \tag{5.6}$$

where R_{0i} is the reference resistance for which S-parameters are determined. Using equation (2.7), the S-parameters can be computed as

$$S_{ij} = \left. \frac{b_i}{a_j} \right|_{a_k = 0, k \neq j} \tag{5.7}$$

Since the reference resistance, R_{0i} ,is known, it is desired to calculate the current I_i and the voltage V_i to compute the S-parameters using (5.5), (5.6), and (2.7).

To implement this approach in FDTD, a suitable mesh location for the voltage sources is first selected (see Figure 5.2). This location automatically defines the position of the ports. The FDTD source can be represented with the equivalent circuit shown in Figure 5.3, where the internal series resistance has been added as part of the code. The description to consider the internal resistance in the FDTD equations is discussed in [*Luebbers and Langdon*, 1996].

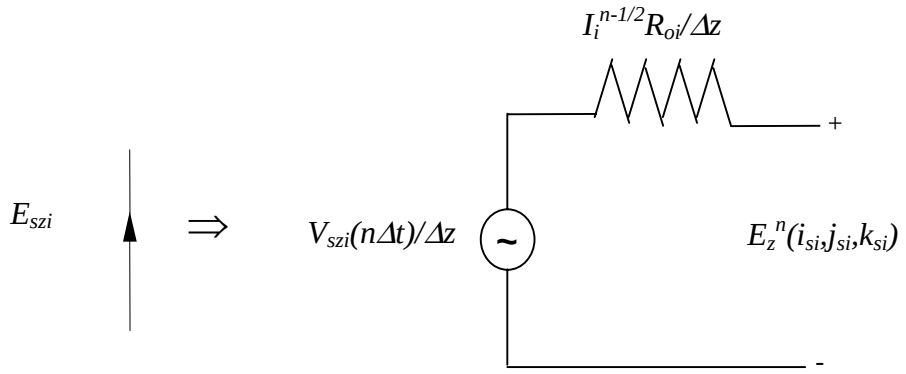

FIGURE 5.3 - Application of FDTD voltage source with internal resistance

To determine the port voltage V_i, the electric field source between the two terminals in Figure 5.3 is calculated as

$$E_z^n(i_{si}, j_{si}, k_{si}) = V_{si}(n\Delta t)/\Delta z - I_i^{n-1/2} R_{0i}/\Delta z \tag{5.7}$$

where the current through the source, I_i, is determined using Ampere's law as

$$\begin{aligned} I_i^{n-1/2} = &\left(H_x^{n-1/2}(i_{si}, j_{si}-1, k_{si}) - H_x^{n-1/2}(i_{si}, j_{si}, k_{si})\right)\Delta x + \\ &\left(H_y^{n-1/2}(i_{si}, j_{si}, k_{si}) - H_y^{n-1/2}(i_{si}-1, j_{si}, k_{si})\right)\Delta y \end{aligned} \tag{5.8}$$

Finally, the voltage, V_i, is calculated multiplying $E_z^n(i_{si}, j_{si}, k_{si})$ in equation (5.7) by Δz. The voltages and currents at each port are recorded and transformed to the frequency domain using a Fast Fourier Transform (FFT) algorithm. Then, equations (5.5) and (5.6) with (2.7) are applied to compute the S-parameters.

In XFDTD, the user defines all the ports in the circuit by selecting the position of the voltage sources. To calculate the S-parameters with respect to an incident wave in port 1 (column #1 of the scattering matrix), the source at this port has to be activated while all the other sources remain "off". At the ports where the source was deactivated (E_{szi}=0), only the 50Ω internal resistance remains connected to ground and the ports are properly matched. Therefore, the internal resistance works as a port termination, which is required by definition to compute the S-parameters. In [*Langdon* et al., 1998], results using this method are shown for different stripline and microstrip structures. The computed FDTD S-parameters show an excellent agreement with measured data.

5-4 Transition from source to microstrip line

It has been observed after hundreds of hours of simulation, that the transition between the source and the input microstrip line plays an important roll when computing the S-parameters with FDTD. For this reason, a section considering only this transition is included in this work.

In some of the cases presented here, it was observed that computed values for S_{11} using FDTD can differ by as much as 20 dB when changing the geometry of the transition alone. This inconsistency in the computation of some of the S-parameters is not acceptable for the simulation, especially if real world measurements are trying to be predicted. This problem was particularly observed at ports where low energy levels are expected. This is the case of a circuit with a 50 Ω input impedance where computed values for S_{11} are expected to be low (ideally -∞ dB), and the case of a directional coupler where very low energy levels are also expected at the isolated port. If the energy level at a particular port is not extremely low (for example the output of a 3dB power splitter) the geometry of the transition does not seem to affect the computation of the S-parameter at this particular ports.

Originally, a tapered line similar to the one in Figure 5.4 was thought to be the proper way to feed the microstrip line, and this actually gives good results for structures like, the patch antenna, branch line couplers, and the Wilkinson power divider. These structures are characterized because of their narrow bandwidth which implies the existence of a well define single resonance frequency that dominates the

output response (point with low energy level). A notch in the S_{11} plot is generally observed at this particular frequency point. The FDTD method has provided excellent agreement between measured and computed data for these narrowband structures when the tapered line transition is used. For structures with a broadband response, such as the coupled line coupler, the Lange coupler, and even a simple 50Ω microstrip line, the transition from Figure 5.4 did not provided acceptable results for S_{11} and the isolated port. However, the other computed parameters (high energy level) still provided good predicted values. To try to solve this problem, a series of FDTD runs were performed using different kind of transitions and computed results were compared to measurements.

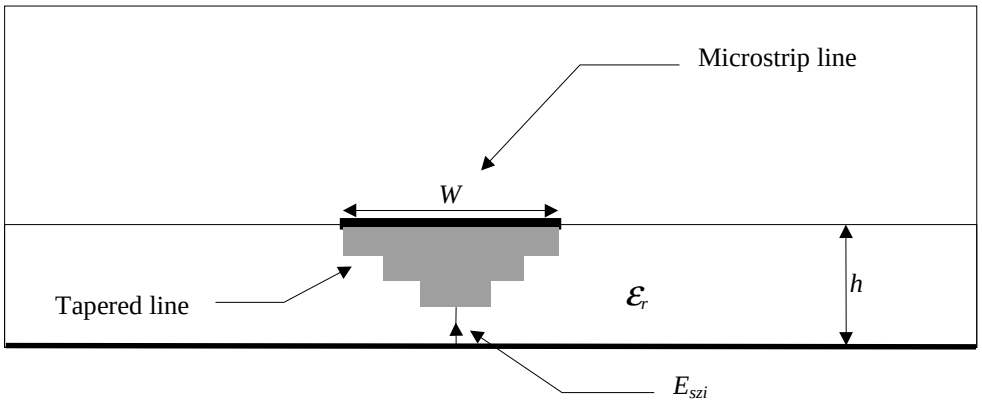

FIGURE 5.4 - Transition from source location to microstrip conductor using tapered line.

In order to create a trustworthy model for the Lange coupler, it is imperative that good results for the four S-parameters are computed with the FDTD simulations. The first step in solving this problem was to find a simple structure that will give a low S_{11} over a broad frequency range. The logical choice is to simulate a simple 50 Ω microstrip line.

Several transitions were tested to feed two different 50 Ω lines. One of the lines was fabricated on a 75 mils thick teflon substrate with ε_r = 6.15. The second line was fabricated with a Teflon substrate with a thickness of 45 mils and ε_r =2.33. The S-parameters were measured with the network analyzer and compared to simulated results obtained for different type of transitions. It is worthwhile to mention at this point that the lines simulated with FDTD during this experiment were 10 to 20 cells wide and the cells ratio

between the width of the line and the thickness of the substrate was between 1.2 to 1.5, which indicates that a high spatial resolution (small Δx, Δy, and Δz) was used for these cases. This high resolution was desired so that the 50 Ω lines previously mentioned are comparable in cell size to the 50 Ω port lines used to feed the Lange coupler and the multilayer structure analyzed in this work. The use of many cells to simulate the 50 Ω port lines is hard to avoid because of the extremely narrow line widths and spacings used in the design of the Lange coupler. At least two cells are required to properly simulate the line width and the spacing between lines. The maximum spatial increment size is then basically limited to small fractions of λ for the construction of the whole structure. The use of different spatial increments using sub-griding techniques could alleviate this problem, but that particular approach was not followed in this work. In some simulated structures presented here, the spatial increments are around $1/250^{th}$ or less of a λ for the higher frequency of interest.

The conclusions for the two experiment with the 50Ω line were similar. A tapered line segment used as a transition did not provide good results for the high resolution lines. A simple straight line consisting of a few cells provided a much better result for S_{11} and the isolated port. This transition is illustrated in Figure 5.5. In some cases, the change in S_{11} by replacing the tapered line transition for the straight line improved the computed results for as much as 20 dB. A comparison of computed versus measured results for both 50Ω lines using different transitions is presented in the next chapter.

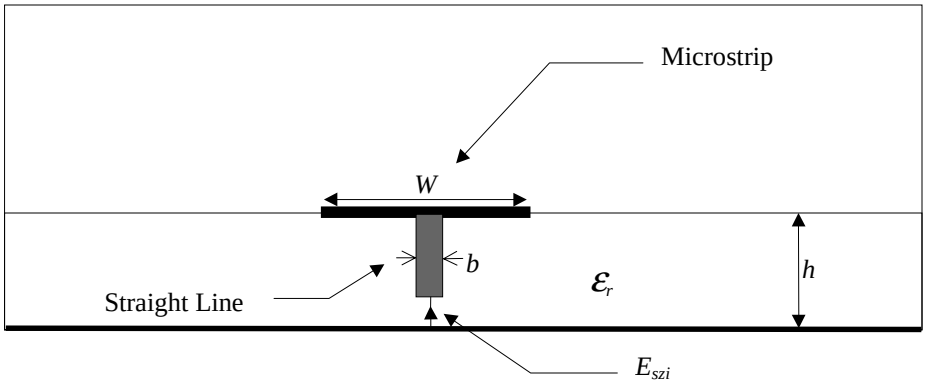

FIGURE 5.5 - Straight transition from source location to microstrip conductor

For the two lines under consideration, it was observed that in order to obtain good results the cells ratio between the width of the line and the width of the transition (*W/b*) has to be between 4 and 6. The

ratio tends to decrease towards 4 when more cells are used to simulate the width of the line. We believe that this type of transition, as opposed to the taper line, provides better results because there is enough room for the generation of electric fields between the microstrip line and the ground plane at the moment that the signal is launched.

There is obviously an optimum width for the transition, a wide transition blocks the fields formation not allowing the proper launching of the signal along the line while a thin line introduces parasitic inductances that affect the computation of the S-parameters. This transition is an original contribution in this work and it was successfully used in most of the cases to be presented. A comparison of measured versus computed S-parameters for different microstrip structures are shown in Chapter 6.

6. Results for some General Microstrip Structures using FDTD

In order to analyze the Lange and the multilayer coupler with FDTD, the first step was to validate the predicted S-parameters by comparing them to measured data. Measured versus FDTD computed results for the coupled line coupler, the branch line coupler, and the Wilkinson power divider are presented here. The S-parameters for these structures have been successfully predicted using different approaches [*Sheen* et al., 1990; *Shibata and Kimura*, 1993; *Yu*, 1997; *Lin and Naishadham*, 1994], but in this work the new technique discussed in Chapter 5 is implemented.

Results for the Lange coupler are also presented here, and presently there is no documentation in the literature of this structure being modeled using FDTD. Results for a 50 Ω line are also presented in this section. Even though the input impedance and effective dielectric constant for a 50 Ω microstrip line have been successfully predicted using FDTD [*Sheen* et al., 1990*; Shibata and Kimaru*, 1988; *Bi* et al., 1992], there is no formal comparison of the predicted and measured S-parameters for such a line in the literature.

In this work, excellent agreement between measured and computed S-parameters for the 50Ω line is presented for the first time. Other computed FDTD results concerning the multilayer and special cases for the Lange coupler are also original and results are presented later when a complete analysis is performed for each case. The geometry of each of the structures is constructed following the considerations for microstrip analysis discussed in Chapter 5.

6-1 50 Ohms Microstrip Transmission Lines

The two simulated 50 Ω lines presented here were a very important step in the completion of this work. The main goal was to find the right transition to properly launch the signal into the microstrip circuit. It is shown here that the straight transition from Figure 5.5 provided the best results predicting S_{11}. The results built the necessary confidence to implement this transition with the interdigitated structures to

be analyzed later. The first line was fabricated on a 62 mils substrate material with $\varepsilon_r = 2.33$. The line has a width of the 4.572 mm and is 25.4 mm long. The dimensions for the line are shown in Table 6.1. The last column from the table shows the FDTD dimensions after the ½ cell correction has been applied. The geometry for the FDTD meshed line is shown in Figure 6.1. Figure 6.2 shows the computed and measured S-parameters of the 50 Ω line, it is evident that the agreement is excellent. This is the first time that S-parameters results for a 50 Ω line using FDTD are reported. In [*Sheen* et al., 1990] and [*Lin and Naishadham*, 1994] a simulated 50Ω microstrip line provides excellent agreement when the input impedance is compared to measurements. *S*-parameters for the line were not reported in either case.

With this transition, we were able to match the input impedance as well as the *S*-parameters of the line for a frequency range up to 15 GHz. The transition used for this particular line is shown in Figure 6.3. The transition is two cells wide and the ratio between line and transition width is 4.

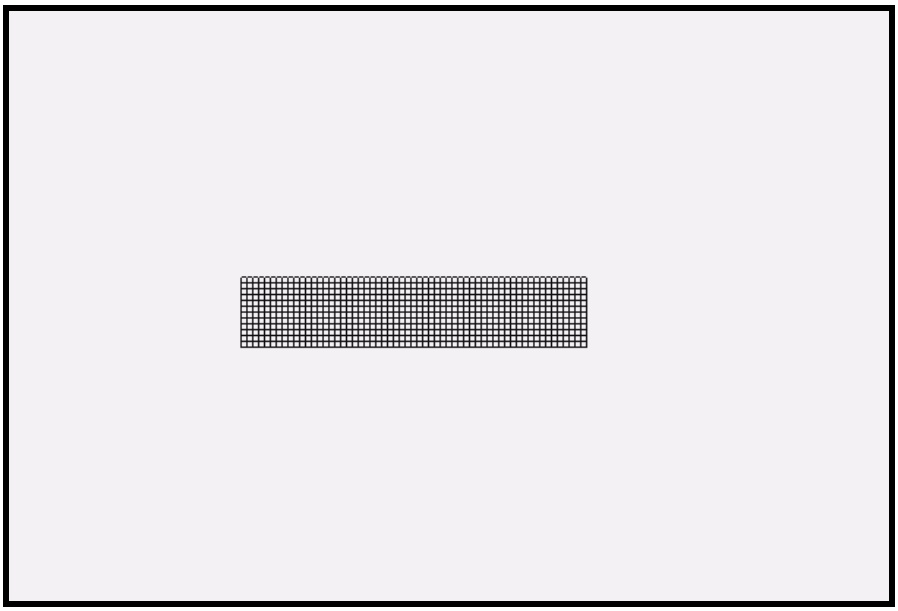

FIGURE 6.1 - FDTD geometry for 50 Ω line with h=62 mils, ε_r=2.33.

TABLE 6.1 - Physical and FDTD dimensions for 50Ω line with h=62 mils, ε_r=2.33.

	Physical Dimension	FDTD Cells	FDTD Dimension
W (mm)	4.572	12Δy	4.576
l (mm)	25.4	65Δx	23.49
$h_{substrate}$ (mm)	1.57	8Δz	1.57
FDTD Cell Space: $150 \times 101 \times 100$; Cell size: Δx=356 , Δy=352 Δz=197 μm. FDTD Excitation: Gaussian Derivative; Pulse Width: 160; Time Steps: 1600			

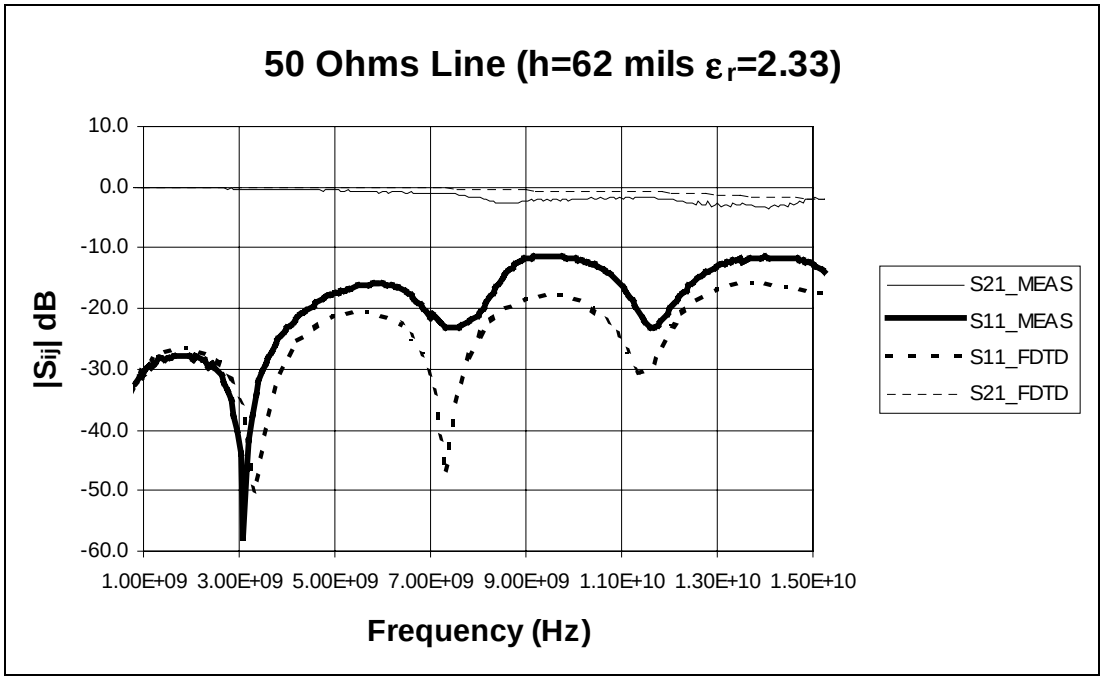

FIGURE 6.2 - S-parameters for 50 Ω line with h=62 mils, ε_r=2.33.

The same line was also simulated using higher resolution and the results were excellent when using the same type of transition. For lines where the resolution was low (6 cells wide or less) this transition did not provide a good agreement with measurements. In our case, an FDTD volume with high resolution is required to simulate the structures of interest, and the straight transition was always used with excellent results.

A second line fabricated on a 75 mils substrate with ε_r =6.15 was also measured and simulated with FDTD. The simulation approach was the same followed for the first line and excellent results were also obtained using the straight transition.

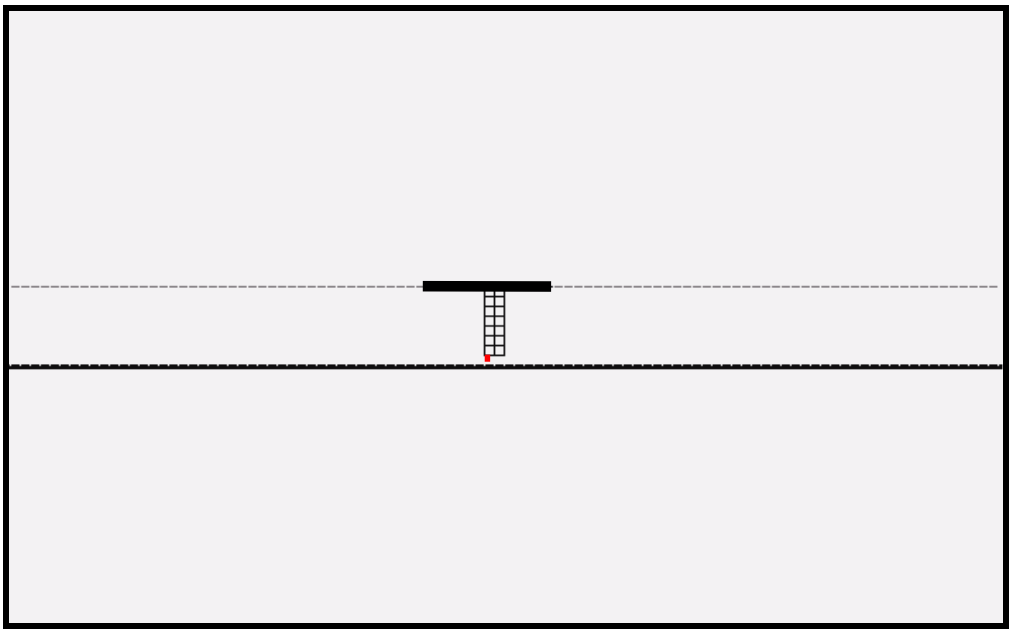

FIGURE 6.3 - FDTD transition for 50 Ω line with h=62 mils, ε_r =2.33.

The width of the transition was meshed in FDTD using 3 cells. The dimensions for the second line are given in Table 6.2 and the results are shown in Figure 6.4. The results are excellent up to 11 GHz. For comparison purposes, the same line was simulated using the taper line transition similar to the one in Figure 5.4. The results using the taper line transition are shown in Figure 6.5. It is evident from the figure that a dramatic improvement in the S-parameters is obtained when the straight line transition approach is used.

TABLE 6.2 - Physical and FDTD dimensions for 50Ω line with h=75 mils, ε_r =6.15.

	Physical Dimension	FDTD Cells	FDTD Dimension
W (mm)	2.794	12Δy	2.8
l (mm)	25.4	59Δx	25.37
$h_{substrate}$ (mm)	1.57	8Δz	1.57
FDTD Cell Space: 150 × 101 × 100; Cell size: Δx=430 , Δy=216 Δz=238 μm. FDTD Excitation: Gaussian; Pulse Width: 160; Time Steps: 5000			

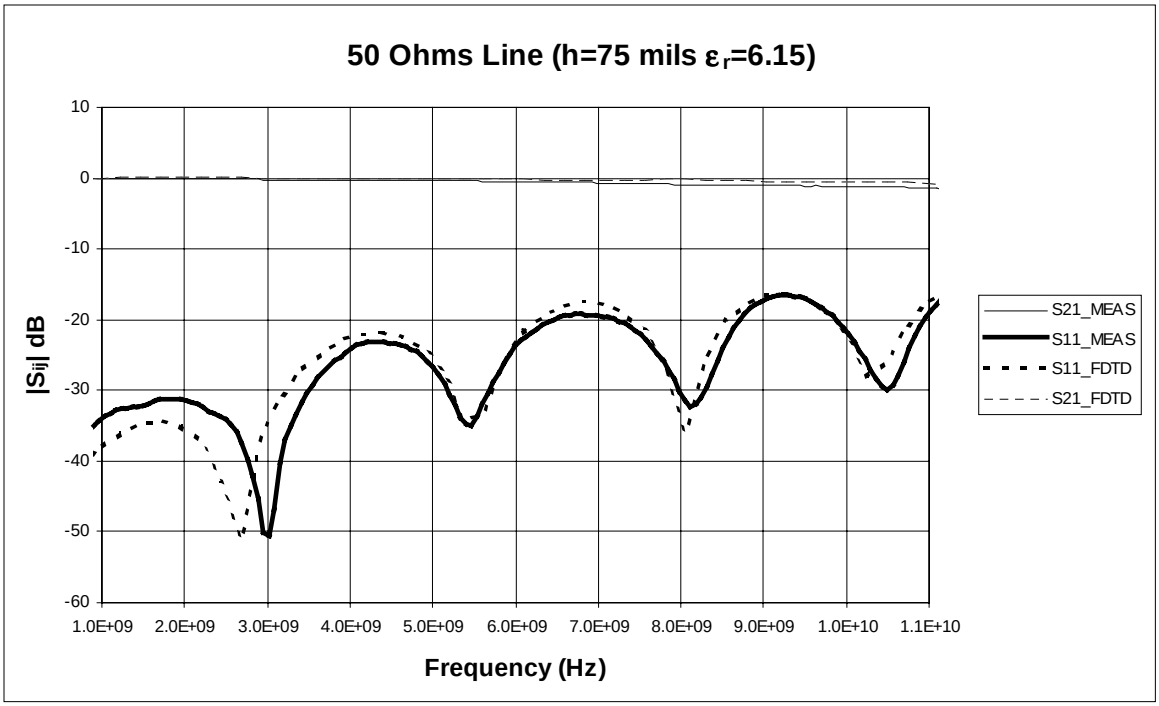

FIGURE 6.4 - S-parameters for 50Ω line with h=75 mils, ε_r=6.15

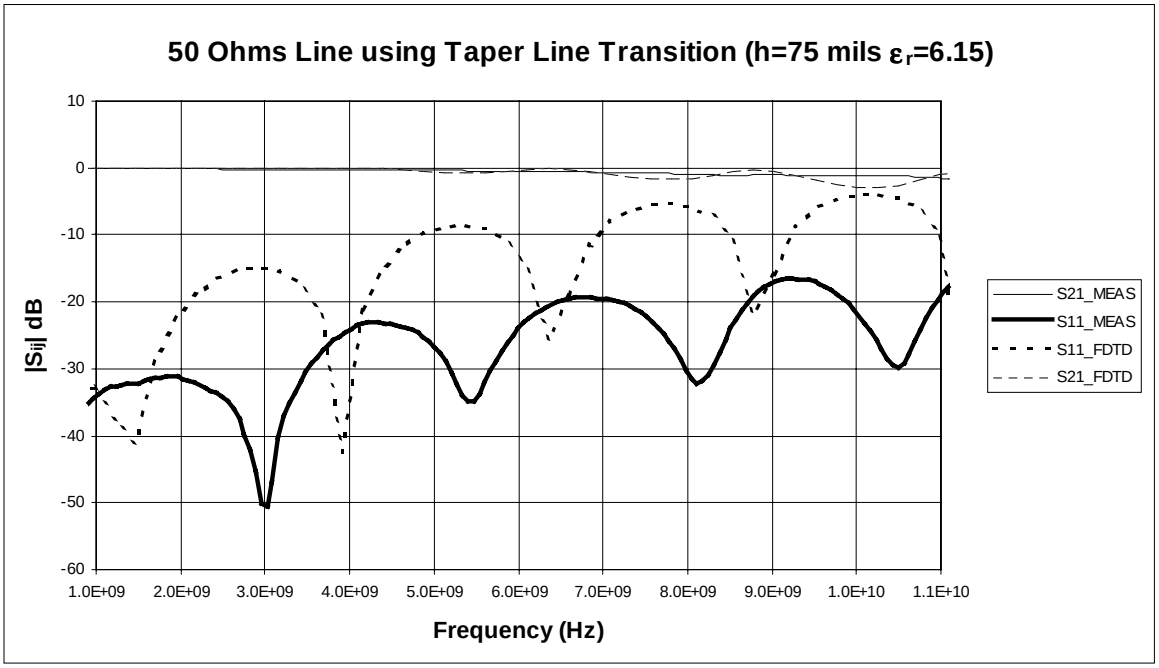

FIGURE 6.5 - S-parameters for 50Ω line with h=75 mils, ε_r=6.15 when taper line is used as transition.

The second line discussed here was also simulated with higher resolution, the width of the line was modeled using 20 cells in one case and 34 cells in another case. The spatial resolution was adjusted so that the 2:1 ratio between spatial increments was not exceeded. The transition was also changed so that the ratio between the width of the line and the transition width was approximately the same for all the cases. The computed S-parameters for the two higher resolution cases were almost identical to the results shown in Figure 6.4. The only disadvantage observed with this transition was that at very high frequencies the FDTD simulation seems to fail. This effect can be observed in Figure 6.6, where the frequency response for the 75 mils line is plotted up to 26.5GHz.

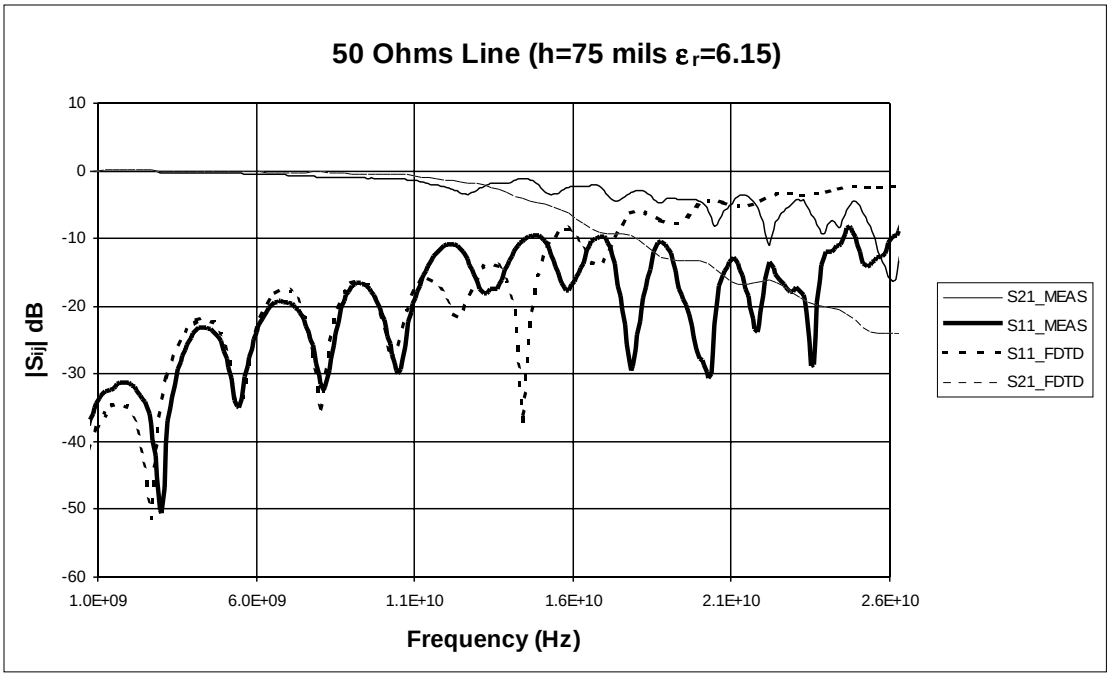

FIGURE 6.6 - S-parameters for 50Ω line with h=75 mils, ε_r=6.15

In Figure 6.6 it is observed that the S-parameters computed with FDTD are moving away from the measurements at about 15 GHz. The same effect was also observed for the 62 mils line at about 25 GHz. This discrepancy at higher frequencies with the FDTD results does not present a practical problem since thick substrates (62 and 75 mils are considered thick) are usually avoided for high frequency applications. Thin substrates are more commonly used at high frequencies to avoid higher losses and the danger of propagating surface waves, and to minimize dispersion effects. The thin substrate is also required when

miniature circuits are desired which has become a common and desired practice. The effect shown in Figure 6.6 is less pronounced when structure on thin substrates materials are simulated with FDTD. Later in this work, a simulation for a 50 Ω line on a 15 mils substrate is presented. The results for this line are valid to frequencies up to 90 GHz.

6-2 Coupled Line Coupler

A 3 GHz coupled line coupler similar to the one in Figure 3.6 was constructed in the laboratory. The coupler was designed for a coupling factor of 20 dB and it was fabricated on a substrate that has a dielectric permittivity of 2.33 and a total dielectric thickness of 1.143 mm. Figure 6.7 shows the FDTD geometry used to simulate the coupled-line coupler. The FDTD cell size is Δx=373.4μm, Δy=373.4μm, Δz=228.6μm. The total FDTD cell space is $115 \times 200 \times 50$ cells. The physical dimensions and the FDTD equivalent in cells size are given in Table 6.3. The last column gives the FDTD dimensions after applying the ½Δ correction. The electric field mesh located on the surface of the substrate are assigned a dielectric constant of (2.33+1)/2=1.67 to accurately model the air/dielectric interface in the FDTD equations. As Table 6.3 shows the cell size Δz was chosen to match the substrate thickness exactly when 5 cells are used.

TABLE 6.3 - Physical and FDTD dimensions for the coupled line coupler.

	Physical Dimension	FDTD Cells	FDTD Dimension
W (mm)	3.302	8Δy	3.36
S (mm)	1.473	5Δy	1.49
$l_{\lambda/4}$(mm)	17.78	48Δx	17.92
W_{port}(mm)	3.38	8Δx	3.36
l_{port}(mm)	12.7	34Δy	12.69
$t_{substrate}$(mm)	1.143	5Δz	1.143
FDTD Cell Space: $115 \times 200 \times 50$; Cell size: Δx=373.4 , Δy=373.4 , Δz=228.6μm. FDTD Excitation: Gaussian; Pulse Width: 64; Time Steps: 3500			

S-parameter measurements for the coupler were collected using a network analyzer. Measurements are plotted in Figure 6.8 and compared to FDTD results. The figure shows a good agreement between the measured and simulated results.

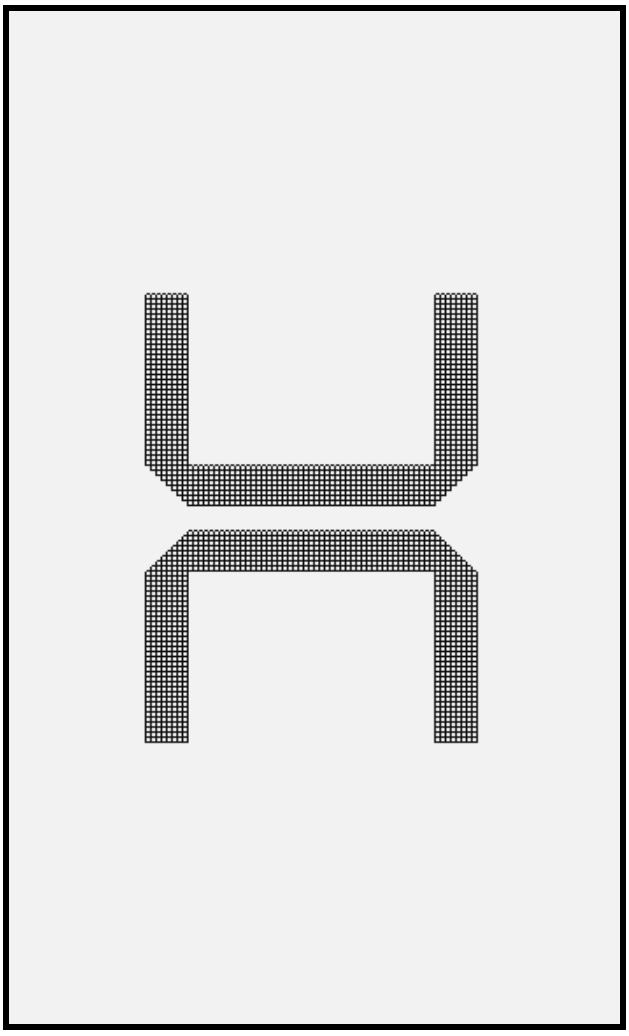

FIGURE 6.7 - FDTD geometry for the coupled line coupler

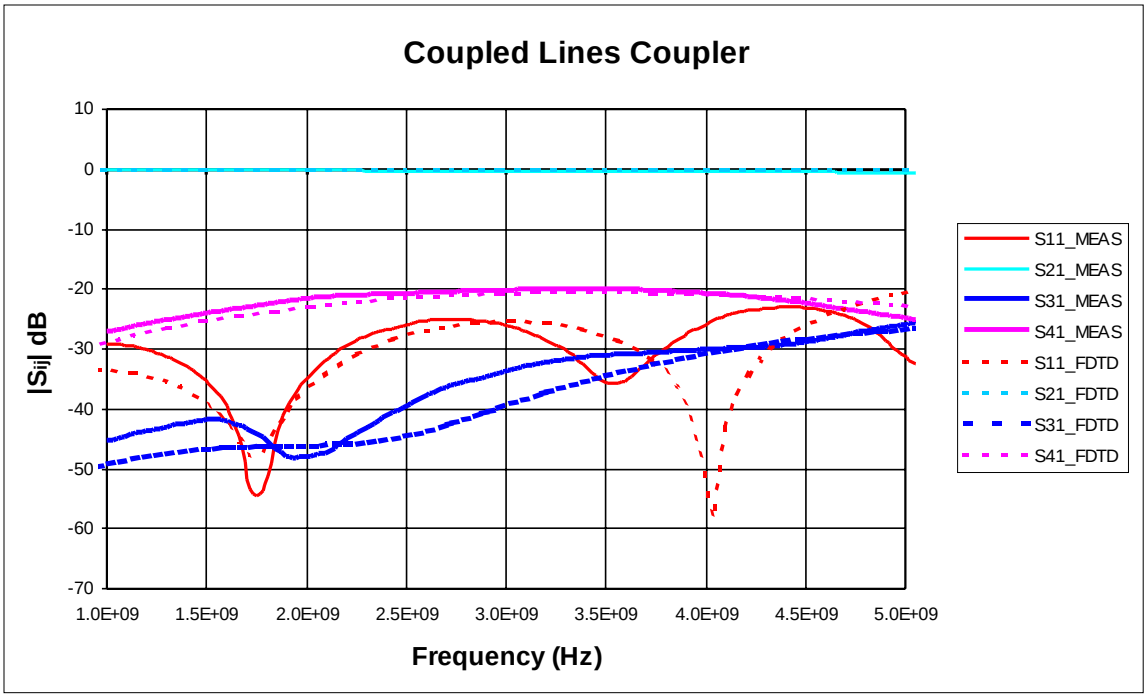

FIGURE 6.8 - Computed versus measured S-parameters for the coupled line coupler.

Not many results for structures with continuos coupling, like the coupled line coupler, are available in the literature. In [*Sheen*, 1988], a similar coupler with a center frequency of 8 GHz is simulated. A good agreement for S_{21}, S_{31}, and S_{41} was reported for this case. Sheen also predicted an S_{11} below 20 dB from 1 to 16 GHz, which is an indication of a good match, yet the low level resonance points computed with FDTD did not match the measurements.

If we compare our results over an equivalent 2:1 frequency bandwidth, we can conclude that a better agreement for S_{11} was obtained here. From the Figure 6.8, a good agreement is observed at the first resonance shown by S_{11}. In addition, it is observed that a second resonance at 3.5 GHz was predicted 500 MHz higher by FDTD. This is not considered a major problem since the dB levels are comparable for the computed and measured data, implying that the computation of the input impedance of the system is practically not affected. The other S-parameters show an excellent agreement, any minor discrepancies in the results can be attributed to the fabrication procedure.

6-3 Branch Line Coupler

A 3 dB branch line coupler with f_c=3 GHz was also fabricated on a substrate that has a dielectric permittivity of 2.33 and a total dielectric thickness of 1.143 mm. To achieve the 3 dB coupling the dimensions for the line widths are calculated for the case when Z_{series}=35.4 Ω and Z_{shunt}=50 Ω. This case was previously discussed in section 3.1. The physical dimensions and the FDTD dimensions used for this simulation are shown in Table 6.4. The assignment of variables from this table correspond to the layout shown in Figure 3.3. Figure 6.9 shows the FDTD geometry used in the simulation of the branch line coupler.

TABLE 6.4 - Dimensions for the branch line coupler.

	Physical Dimension	FDTD Cells	FDTD Dimension
W_1 *(mm)*	5.54	17Δy	5.526
W_2 *(mm)*	3.38	10Δx	3.38
$l_{\lambda/4}$*(mm)*	17.78	58Δx	17.81
W_{port}*(mm)*	3.38	10Δy	3.38
l_{port}*(mm)*	17.8	58Δx	17.81
$t_{substrate}$*(mm)*	1.143	3Δz	1.143
FDTD Cell Space: 235 × 125 × 20; Cell size: Δx=307 , Δy=307 , Δz=381μm. FDTD Excitation: Gaussian; Pulse Width: 64; Time Steps: 3500			

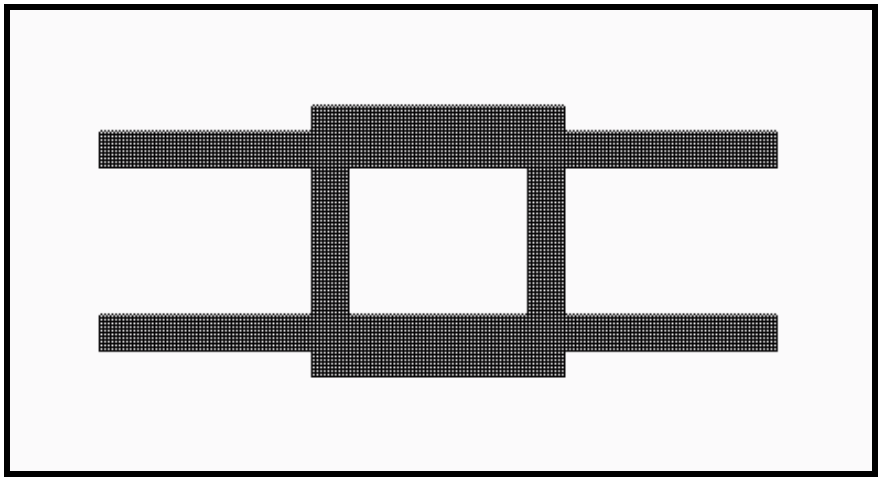

FIGURE 6.9 - FDTD geometry for branch line coupler.

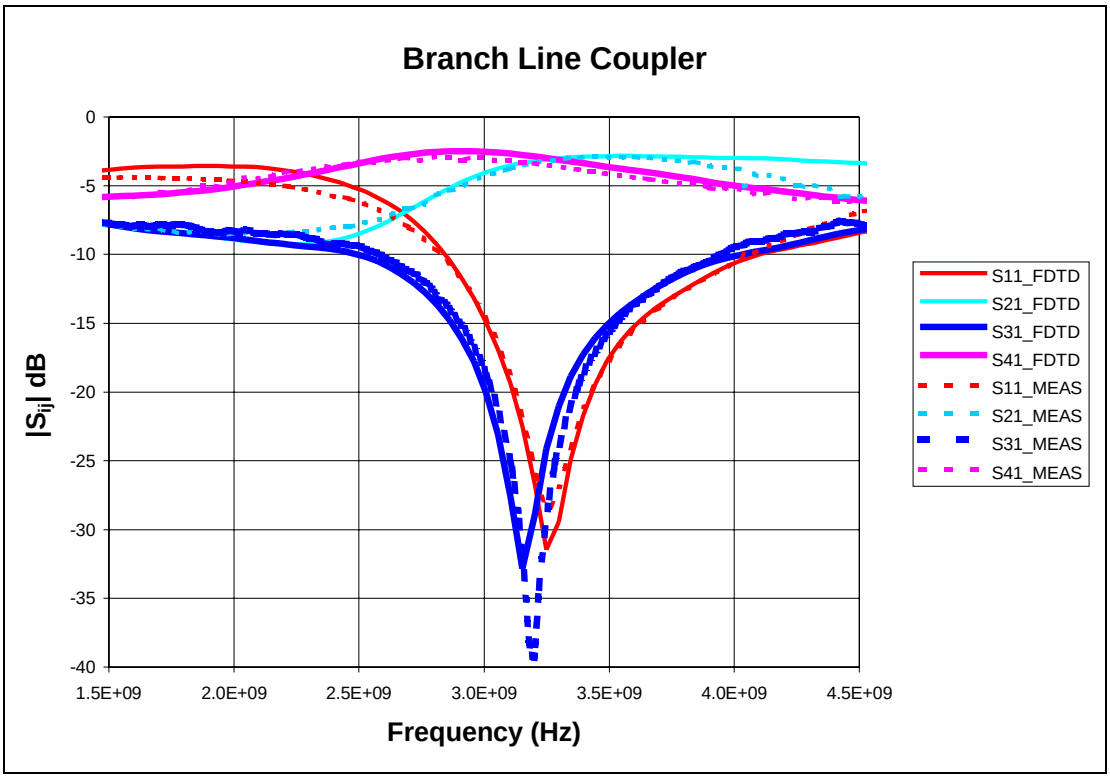

FIGURE 6.10 - S-parameters results for branch line coupler.

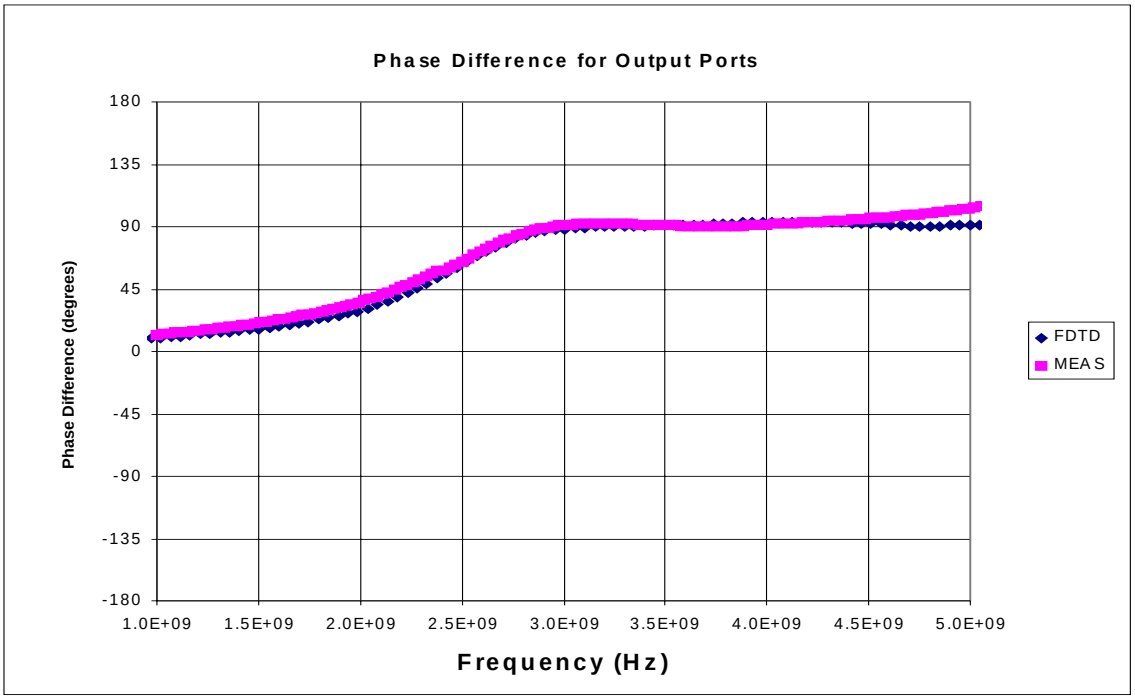

FIGURE 6.11 - Phase difference between output ports for the branch line coupler.

Results for simulated and measured data are plotted in Figure 6.10. The phase difference between the two output ports is plotted in Figure 6.11. For both cases there is also an excellent agreement between both measured and the FDTD results. This type of structure has also been simulated in [*Sheen* et al., 1990] with excellent results.

6-4 Lange Coupler

A simulation of a 3 GHz Lange coupler was also attempted using FDTD. Most of the geometry follows the specifications given by the structure designed by Lange in 1969. Lange provided information for the substrate material, width, and spacing. Figure 6.12 shows the FDTD geometry of the 3 dB Lange coupler constructed with XFDTD. The coupler was fabricated on a substrate with a dielectric permittivity of 10.0 and thickness of 1.067 mm. The 50 Ω port arms were extended 0.779 mm and a spacing of 30 FDTD cells was left between the end of the ports and the FDTD boundaries. The physical and FDTD dimensions of the structure are given in Table 6.5. Note that the length of the structure was not reported in [*Lange*, 1969], and *Linecalc* [*HP-EEsof*, 1996] was used to obtain this parameter.

The dielectric material was set to take the lowest portion of the FDTD volume ($14\Delta z$), while the fields above this portion were set to free space. The microstrip metallization was simulated by assigning a PEC material to the corresponding electric fields on the dielectric/air interface. Other fields at this interface received an averaged dielectric constant of (10+1)/2=5.5.

The bonding wires connecting the alternate lines were also simulated with PEC lines. To simulate the ground plane, the electric fields at the bottom wall of the FDTD volume (x-y plane, k=1) were also set to PEC. The other five walls are simulated as an unbounded space by applying the Liao boundary conditions. Finally, a modulated Gaussian pulse in the +z direction is used for excitation. This pulse knocks down energy that was trapped in the structure oscillating at undesired frequencies. The desired pulse resulted in a width of 10,500 time steps which considerably decreased the running time of the simulation. The source is applied by forcing a +z directed electric field on the FDTD mesh at the closest point normal to the ground plane and centered with respect to the microstrip line width. The source is

connected to the 50 Ω line port using a 3-cell wide straight transition similar to the one discussed in section 5.4.

TABLE 6.5 - Dimensions for the 4-finger Lange coupler

	Physical Dimension	FDTD Cells	FDTD Dimension
W (mm)	0.1143	2Δy	0.114
S (mm)	0.0762	3Δy	0.076
$l_{\lambda/4}$(mm)	10.287*	135Δx	10.26
W_{port}(mm)	0.991*	12Δx	0.988
l_{port}(mm)	**	20Δy	0.779
$t_{substrate}$(mm)	1.067	14Δz	1.067
FDTD Cell Space: $220 \times 200 \times 35$; Cell size: Δx=76 , Δy=38 , Δz=76.2μm. FDTD Excitation: Mod Gaussian; PW: 10,500; TS: 21500; f_c=3GHz			

*Values obtained with *Linecalc* **Not available

The computed S-parameters are compared to experimental data from [*Lange*, 1969] in Figure 6.13. The agreement is considered excellent. The maximum difference between S_{21} and S_{31} is less than 0.2 dB. The return loss (S_{11}) is also below the measurement reported by Lange, which indicates a good match. The predicted isolation (S_{41}) is also excellent, below -25 dB from 2 to 4 GHz, but measurements were not published and they are not included in the figure. The phase difference between the two output ports was also computed with FDTD and there is a maximum variation of 1.35^0 from 90^0 within the 2 to 4 GHz bandwidth. Lange reported a maximum variation of 2 degrees for his structure. The phase difference computed with FDTD is plotted in Figure 6.14.

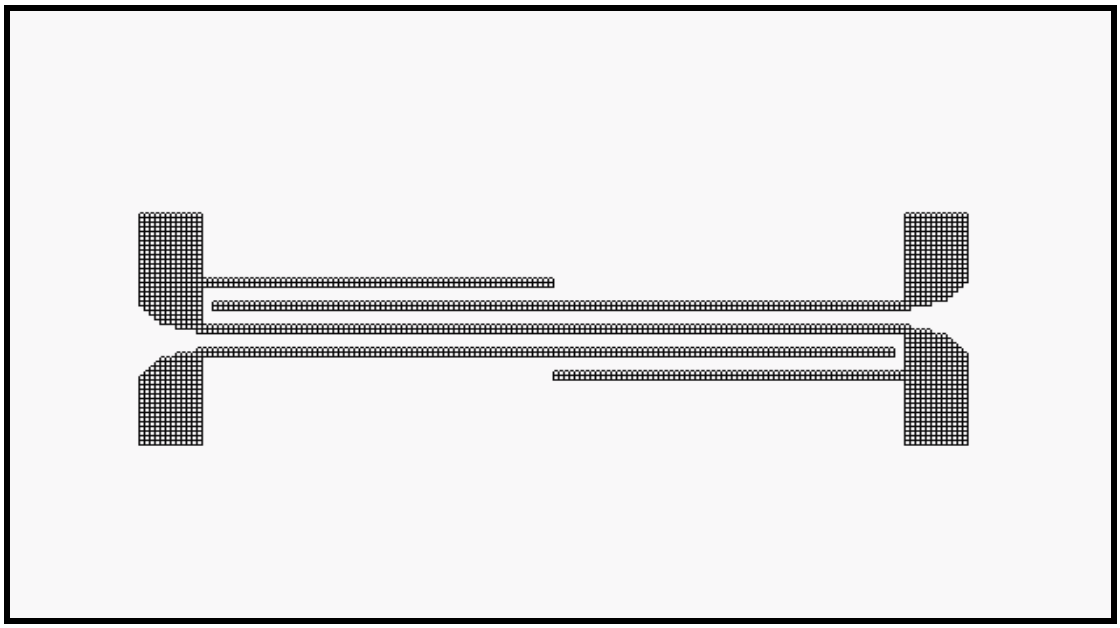

FIGURE 6.12 - FDTD geometry for 4-finger Lange coupler.

These results are considered one of the most important achievements in this work. Figure 6.13 is the strongest proof that the simulation of this structure is possible with FDTD. Presently, there is no indication in the literature that this structure or any other interdigitated hybrid has been successfully simulated with FDTD. This is the first time that results for a microstrip interdigitated coupler are presented.

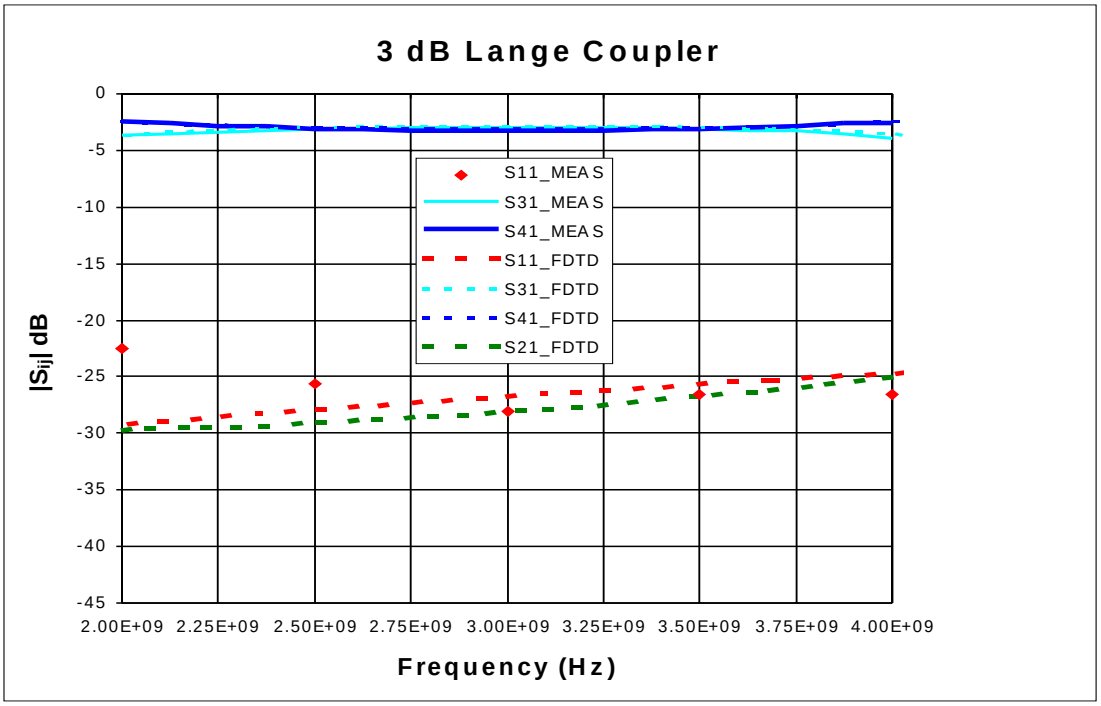

FIGURE 6.13 - S-parameters results for the Lange coupler, dimensions and measurements taken from [*Lange*, 1969].

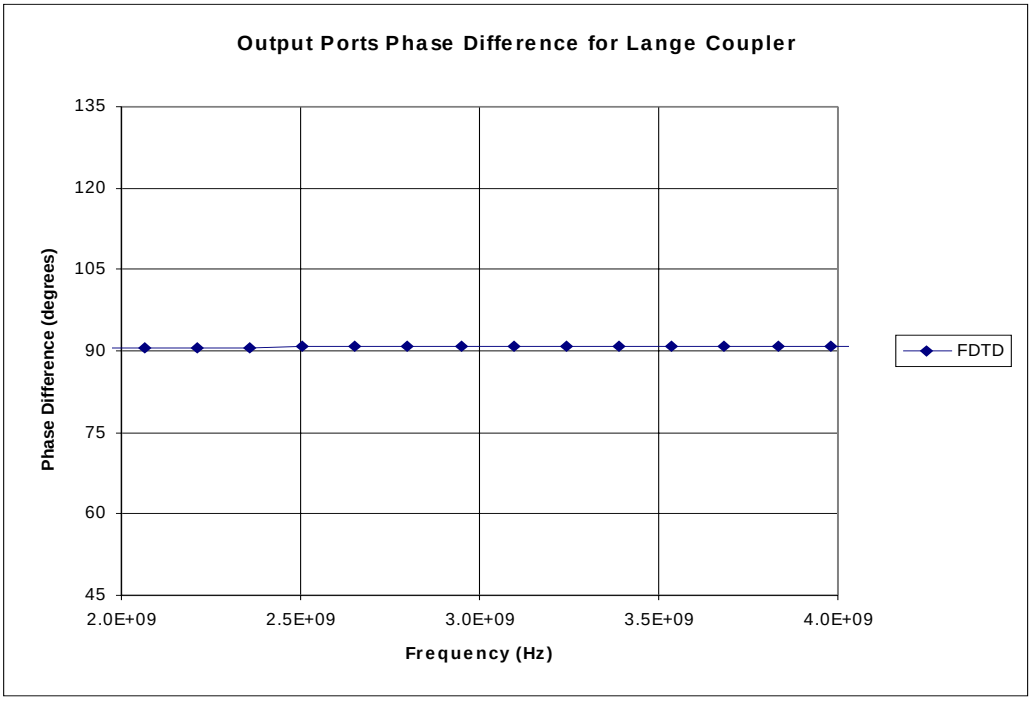

FIGURE 6.14 - Phase difference between two output ports of Lange coupler .

6-5 Wilkinson Power Divider

The simulation of a 3 dB Wilkinson power divider is also included in this section. The layout for this structure is shown in Figure 6.15. This type of divider is a three port structure that provides an equal power split between the two output ports (Port 3 and Port 4) located at the right side. It is not considered a quadrature hybrid since there is not a 90 degrees phase difference between the two output ports, however, the 90 degrees phase shift could be obtained if one of the output port lines is $\lambda/4$ longer.

The input port or Port 1, located at the left side, is a 50 Ω line with a width W_{input} that splits into two thinner lines with characteristic impedance of 70.7Ω with their widths given by W_{output}. The length of the two high impedance lines is a $\lambda/4$ from the center frequency. The gray rectangle is a 100Ω resistor that was modeled by adjusting the conductivity of the material in that area. The resistor is meshed using one cell thick ($1\Delta z$) of lossy dielectric over an area (xy plane) of $12\Delta x * 26\Delta y$, knowing the dimensions of the volume enclosing the lossy material, the conductivity required to simulate the 100Ω lumped resistor is calculated as 70 Mhos/m. Unequal power splits can also be achieved by adjusting the width of the output lines. The resistor is only used to dissipate power reflected from the output ports. If the structure is properly designed, the three ports should be matched and the resistor can be removed.

The structure was fabricated for operation at 3 GHz on a 45 mils substrate material with ε_r=2.33. The dimension for the physical and FDTD geometry are given in Table 6.6 .

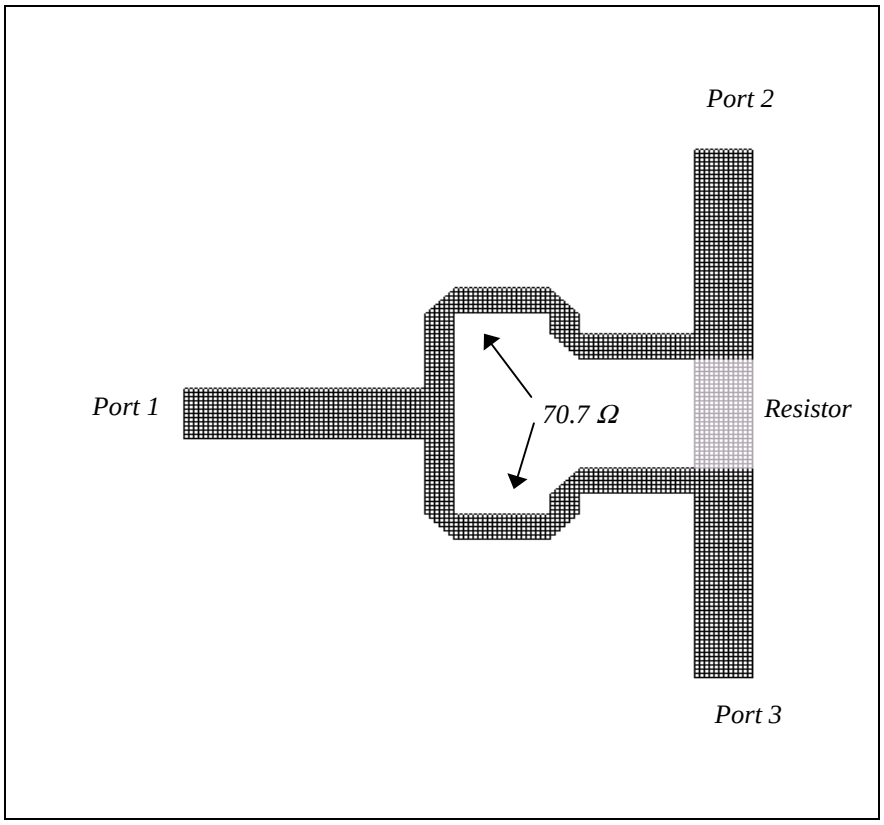

FIGURE 6.15 - FDTD geometry for Wilkinson power divider.

TABLE 6.6 - Physical and FDTD dimensions for the Wilkinson Power Divider

	Physical Dimension	FDTD Cells	FDTD Dimension
W_{ouput} (mm)	17.78	6Δy	18.2
W_{input} (mm)	3.38	12Δy	3.38
$l_{\lambda/4}$ (mm)	19.05	73Δx	18.98
W_{port} (mm)	3.38	12Δx	3.38
l_{port} (mm)	12.446	48Δy	12.48
$t_{substrate}$ (mm)	1.143	8Δz	1.143
FDTD Cell Space: $180 \times 194 \times 41$; Cell size: Δx=260, Δy=260, Δz=142.9 μm. FDTD Excitation: Gaussian Derivative; Pulse Width: 98; Time Steps: 4000;			

The results are shown in Figure 6.16, and again, an excellent agreement is obtained. The figure shows that FDTD accurately predicted the 3 dB power split between the two output ports. This is also shown for the measured data. The predicted S_{11} parameter also shows a good agreement with the measurements. The resonance point is not as pronounced in the measurements as in the FDTD

computations, but this can be due to any imperfections when soldering the connectors to the structure. Similar structures for MMIC applications have been analyzed in [*Gedney* et al., 1996], but the results were not compared to measured data. A stripline Wilkinson power divider is also simulated using this technique, the results agrees with the theory but no experimental data was available [*REMCOM*, 1997].

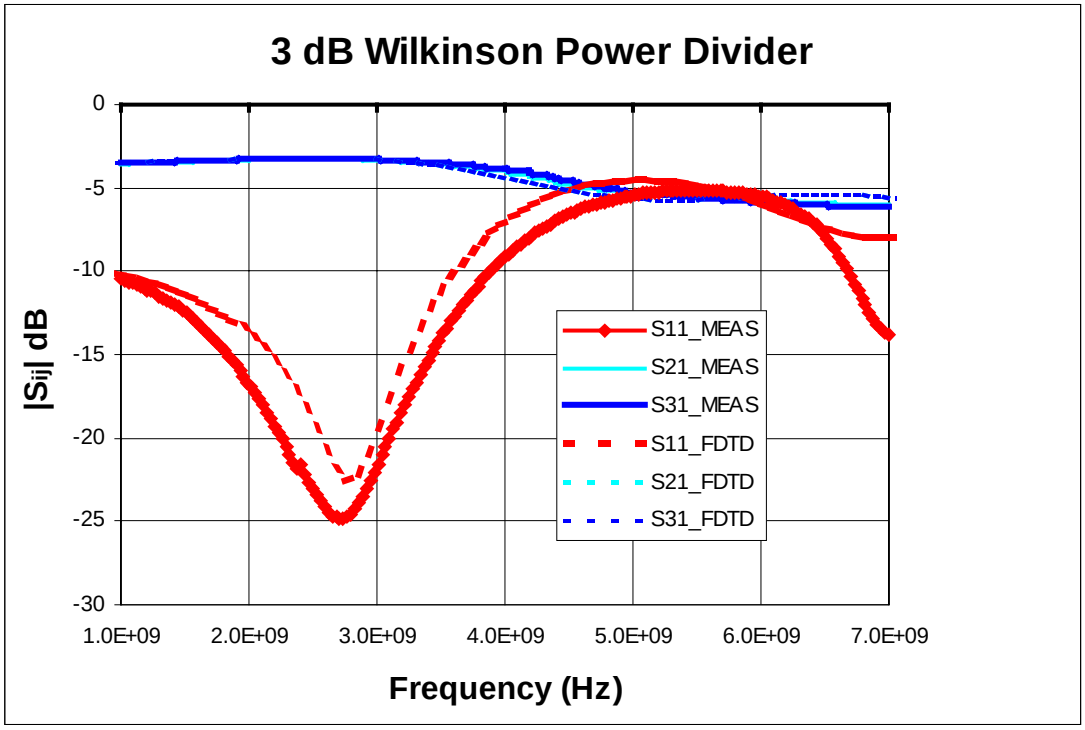

FIGURE 6.16 - S-parameters results for 3 dB Wilkinson power divider.

In this chapter, several microstrip structures were simulated using FDTD. The agreement between computed and measured results were excellent using this approach. Basically, the same considerations presented here will be used for the simulation of the Lange coupler and the multilayer structure when a full analysis is performed. In order to perform a complete analysis that takes into consideration all the controlling parameters of the structure, a powerful statistical technique known as Design of Experiments will be implemented. The next chapter introduces this well known technique and it also discusses the two type of metamodels to be implemented in this work. The chapter also introduces a graphical method to display the output results for the easy identification of an optimum design point.